Stress-assisted large magnetic-field-induced strain in single-variant Co–Ni–Ga ferromagnetic shape memory alloy

2009 J. Phys.: Condens. Matter 21 256002

(http://iopscience.iop.org/0953-8984/21/25/256002)

J. Phys.: Condens. Matter **21** (2009) 256002 (6pp) doi:10.1088/0953-8984/21/25/256002

Stress-assisted large magnetic-field-induced strain in single-variant Co–Ni–Ga ferromagnetic shape memory alloy

H Morito[1], K Oikawa[2], A Fujita[2], K Fukamichi[1], R Kainuma[1] and K Ishida[2]

[1] Institute of Multidisciplinary Research for Advanced Materials, Tohoku University, Katahira 2-1-1, Sendai 980-8577, Japan
[2] Department of Materials Science, Graduate School of Engineering, Tohoku University, Aoba-yama 6-6-02, Sendai 980-8579, Japan

E-mail: morito@tagen.tohoku.ac.jp

Received 20 November 2008, in final form 28 April 2009
Published 1 June 2009
Online at stacks.iop.org/JPhysCM/21/256002

Abstract

The magnetic anisotropy and the magnetic-field-induced strain (MFIS) in a single-variant $Co_{47.5}Ni_{22.5}Ga_{30.0}$ ferromagnetic shape memory alloy (FSMA) have been investigated. From the magnetization curves for the single crystal, the hard c-axis was confirmed, and the uniaxial magnetic anisotropy constant K_u at 300 K was evaluated to be -1.07×10^6 erg cm^{-3} for the single-variant $Co_{47.5}Ni_{22.5}Ga_{30.0}$ martensite phase. The magnitude of compressive shear stress for the variant rearrangement was estimated to be 6.0–7.5 MPa from the stress–strain curves. An assisted stress τ_{assist} of 6.0 MPa was applied before applying a magnetic field, and then a magnetic stress τ_{mag} of 0.3 MPa was added. As a result, a large MFIS of about 7.6 % was obtained at room temperature in the martensite phase of the single-variant $Co_{47.5}Ni_{22.5}Ga_{30.0}$.

1. Introduction

Ferromagnetic shape memory alloys (FSMAs) with a large magnetic-field-induced strain (MFIS) have attracted much attention during the past two decades, because they are promising materials for application in magnetic-field-controlled actuators and sensors. Many kinds of FSMAs have been studied [1–17], in particular, a large MFIS has been observed in Ni_2MnGa alloy in a martensite state phase [1–6]. However, high brittleness of Ni_2MnGa is disadvantageous for practical applications in various fields. Therefore, research and development of ferromagnetic shape memory alloys with excellent improved mechanical properties are strongly needed.

The MFIS of Ni_2MnGa is realized by the rearrangement of martensite variants under the influence of an external magnetic field [1–6]. The thermoelastic martensite phase consists of an assembly of variants arranged coherently during the martensitic transformation. In each variant, the magnetic moment M is pinned in the direction parallel to the magnetic easy axis due to the magnetic anisotropy. The magnetizations in two neighboring variants may be represented by two vectors M_1 and M_2. When a magnetic field H is applied, the magnetization M_1 direction changes its direction from easy axis to the direction of the applied magnetic field. For a large magnetic anisotropy, the angle between M and the applied magnetic field H may be lowered by not only the independent rotation of M but also the variant rearrangement so that both the directions of M and the easy axis approach the parallel direction of H. The applied Zeeman energy $[(M_2 - M_1) \cdot H]$ leads to a driving force on the variant boundaries. When the energy required to move the variant boundaries is low, the magnetization can be turned to the external field direction, changing variants, and hence remaining in the original easy direction in the turned variant [1–6]. Since the MFIS is caused by the martensite variant reorientation, its characteristic behavior is affected by magnetic anisotropy as well as the mobility of variant boundaries [5, 6]. In particular, the magnetic anisotropy energy is required to be larger than the

energy to drive the variant boundaries in order to obtain the MFIS.

Recently, Co–Ni–Ga alloys first reported by Wuttig *et al* [18] have been developed as new FSMAs [18–26]. Oikawa *et al* [19] reported that Co–Ni–Ga alloys in a composition range of Co–(15–30) at.% Ni–30 at.% Ga exhibit both the β ($B2$) to β' ($L1_0$) thermoelastic martensitic transformation and the temperatures, T_{Ms} (martensitic transformation starting temperature), T_{Mf} (its finishing temperature), T_{As} (reverse transformation starting temperature) and T_{Af} (its finishing temperature), and the Curie temperature T_C can be controlled over a wide range of temperatures by changing composition. Furthermore, it is important practically to note that an introduction of a small amount of γ solid-solution fcc phase into the β phase using heat treatment is available to improve the ductility of these alloys [27]. The advantages mentioned above strongly suggest that Co–Ni–Ga alloys are fascinating in the FSMA systems. Although evaluating the magnetic anisotropy and mobility of variant boundaries is important to control the MFIS, because the magnetic anisotropy energy is required to be larger than the energy required to drive the variant boundaries, those data for the Co–Ni–Ga system are, to our knowledge, missing. These intrinsic properties which affect the characteristics of MFIS are caused by the β' phase. Many variants are induced in a self-accommodating manner when the martensitic transformation occurs, resulting in a dispersed state of magnetic anisotropy. Such a multi-variant state prevents us from evaluating the strict value of the magnetic anisotropy constant. Therefore, single-variant specimens are necessary for the precise measurements. In the present paper, the magnetic properties such as magnetic anisotropy, MFIS, and the mobility of variant boundaries have been investigated for a β' phase of the single-variant $Co_{47.5}Ni_{22.5}Ga_{30.0}$ alloy.

2. Experiments

In the present work, taking the previous data into consideration, the alloy composition was set as $Co_{47.5}Ni_{22.5}Ga_{30.0}$ which has both T_C and the martensitic transformation temperatures above room temperature. The single crystals were grown by an optical floating-zone method under a helium atmosphere. Before heat treatment, the crystallographic orientations of the single crystals were determined from electron-backscattering diffractions. The cubic specimens in the parent phase were trimmed so that the $\langle 100 \rangle_P$ (P: parent) directions are parallel to the faces. The single-crystal specimens were annealed at 1473 K for two days to homogenize, followed by quenching in ice water. The martensitic transformation temperature of the specimen was slightly increased by the heat treatment, and confirmed to be in a martensite phase at room temperature. The Curie temperature T_C and the martensitic transformation temperatures for the $Co_{47.5}Ni_{22.5}Ga_{30.0}$ single crystal were confirmed by the thermomagnetization curves in a magnetic field of $H = 100$ Oe and differential scanning calorimetry (DSC) measurements. The phase identification was carried out by x-ray powder diffraction (XRD) using Cu Kα radiation. The powder specimen for XRD measurement was filed from the single crystal and sealed in a quartz capsule, followed by heat-treatment at 1473 K for 15 s to eliminate internal strains.

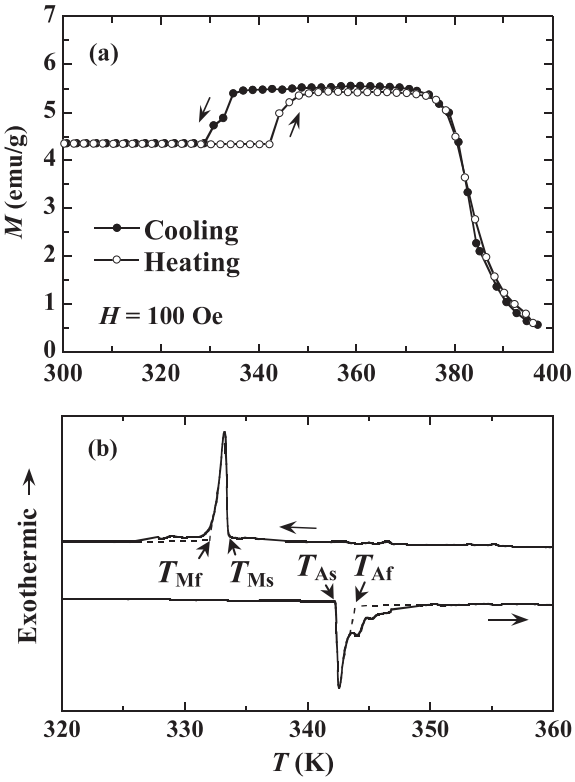

Figure 1. (a) Thermomagnetization curves in a magnetic field of 100 Oe and (b) DSC curves for the cooling and heating processes for the single-variant $Co_{47.5}Ni_{22.5}Ga_{30.0}$ before applying compressive stress.

In order to obtain a single-variant specimen, uniaxial compressive stress was applied to the $[010]_P$ direction in the martensite phase of the above-mentioned single crystals. The magnetization for the single-variant specimens was measured up to 50 kOe with a superconducting quantum interference device (SQUID) magnetometer. The measurement of MFIS was made with an extensometer under a compressive stress in a magnetic field.

3. Results and discussion

3.1. The Curie temperature, martensitic transformation temperatures, and crystal structures

The thermomagnetization curves in the cooling and heating processes are shown in figure 1(a) for the $Co_{47.5}Ni_{22.5}Ga_{30.0}$ single crystal before applying the compressive stress. In the cooling process, the increase in magnetization M due to the transition from the paramagnetic (PM) to ferromagnetic (FM) state is observed around 380 K. In the further cooling, a drastic decrease of M due to the change in the magnetic anisotropy caused by the martensitic transformation is observed around 330 K. As shown in figure 1(b), both the martensitic and reverse transformations exhibit exothermic and endothermic peaks in the cooling and heating processes, respectively. From the thermomagnetization and DSC curves in figures 1(a) and (b), several temperatures are defined as $T_C = 380$ K, $T_{Ms} = 337$ K, $T_{Mf} = 332$ K, $T_{As} = 344$ K, and $T_{Af} = 352$ K.

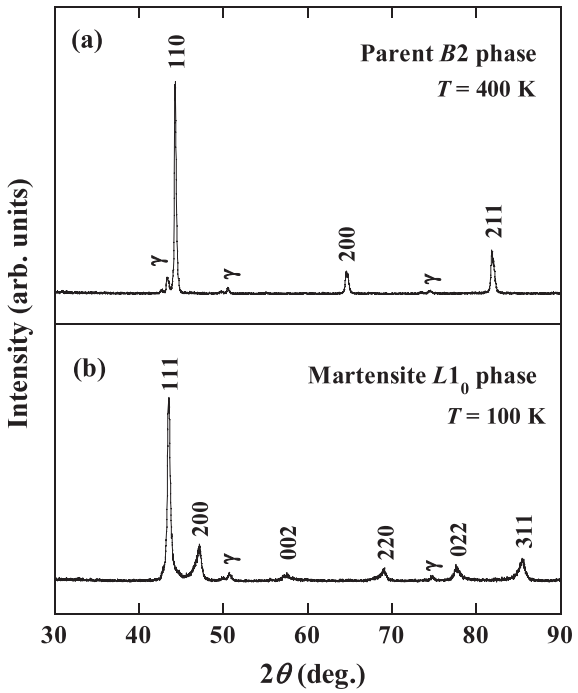

Figure 2. X-ray diffraction patterns at $T = 400$ K for the parent phase and 100 K for the martensite phase in $Co_{47.5}Ni_{22.5}Ga_{30.0}$.

The present single crystal is confirmed to be in a martensite phase at room temperature.

It has been reported that the magnetic anisotropy and the mobility of variant boundaries depend on the crystal structures in Ni_2MnGa [5, 6]. In the present sub-section, the crystal structures of the $Co_{47.5}Ni_{22.5}Ga_{30.0}$ alloy have been investigated. In the powder sample with small grains, the martensitic transformation temperature is decreased by the grain size effect [28]. Therefore, the powder specimen is a mixture of parent and martensite phase at room temperature. In the present study, to identify the parent and martensite phase, the x-ray diffraction patterns were measured at 400 and 100 K, respectively. The peaks of the parent phase obtained at 400 K are identified as the $B2$ structure as indexed in figure 2(a). There are some reflections matched with those of the disordered fcc (γ) phase at $2\theta = 42°$, 50° and 75° in the spectra at 100 and 400 K, although no γ phase was confirmed in the bulk specimen by the optical microscopic observation. The γ phase is considered to be brought about by precipitation during the cooling process, because the cooling rate for the powder obtained by quenching without breaking the quartz tube is lower than that of the bulk specimen quenched in ice water in the present experiments. The x-ray diffraction pattern at 100 K for the martensite phase is well identified as the $L1_0$ structure as indexed in figure 2(b). The lattice parameters of the $B2$ and $L1_0$ structures were determined to be $a_0 = 0.287$ nm and $a = 0.383$ nm, $c = 0.320$ nm. The c/a ratio of the $L1_0$ phase is 0.836, very close to that of $Co_{49.0}Ni_{22.0}Ga_{29.0}$ [22]. The relation of the crystal structures between the parent and martensite phases in Co–Ni–Ga is illustrated in figure 3. The solid and dashed lines represent the $B2$ structure of the parent cubic phase and the $L1_0$ of the

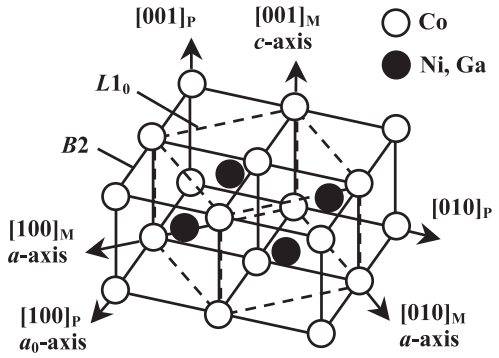

Figure 3. The relation of the crystal structures between the parent and martensite phases in Co–Ni–Ga. The solid and dashed lines show the $B2$ structure of the parent phase and the $L1_0$ of the martensite phase, respectively.

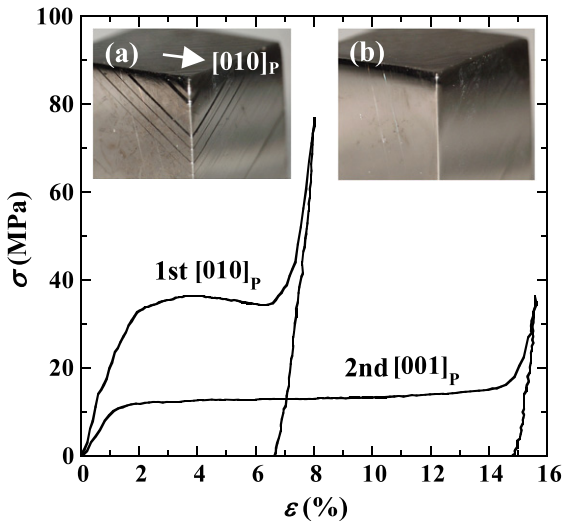

Figure 4. Compressive stress–strain curves along the $[010]_P$ and $[001]_P$ directions at room temperature for $Co_{47.5}Ni_{22.5}Ga_{30.0}$ in the martensite phase. The optical micrographs of the single crystal $Co_{47.5}Ni_{22.5}Ga_{30.0}$ (a) before and (b) after applying compressive stress.

martensite phase, respectively. In the former phase, the $\langle 100\rangle_P$ direction corresponds to either the $[110]_M$ (M: martensite) or the c-axis direction in the latter phase. Transforming from the $B2$ parent phase to the $L1_0$ martensite, the c-axis, i.e. $[001]_M$, produces an expansion of 11.5% relative to the $[001]_P$ direction and the a-axis; $[010]_M$ brings about a shrinkage of 5.6% relative to the $[110]_P$ direction.

3.2. Mobility of variant boundaries

The variant boundary motion under the magnetic field is identical to that under stress, and the mobility of the variant boundaries is related to the twinning stress, that is, the lower the twinning stress, the higher the mobility of the variant boundaries [5, 6]. In order to evaluate the twinning stress, the compressive stresses were applied to the martensite specimens with a cubic shape.

Shown in figure 4 are the room temperature stress–strain curves for $Co_{47.5}Ni_{22.5}Ga_{30.0}$. Since the temperature T_{Af} of the

specimen is 344 K above room temperature and the stresses were applied in the martensite state, the crystal directions are expressed using those of the parent phase. In the first cycle, the compressive stress was applied along the $[010]_P$ direction. The variant rearrangement was initiated above the applied twinning stress σ_{tw} of 35 MPa, corresponding to the level of the plateau in the curve. As a result, the twinning strain ε is evaluated to be about 6.6 %. In the process mentioned above, the *c*-axis is preferentially developed in the direction perpendicular to the compressive direction. By applying a uniaxial compressive stress along the $[010]_P$ direction, the specimen should remain in a multi-variant state because the *c*-axis of the martensite phase aligns itself along the two equivalent directions, i.e. $[100]_P$ and $[001]_P$. In the present alloy system, however, the compressive stress to the specimen yields a single-variant state after the first cycle. The detailed reason is not clear at the present stage, though a preferential growth of one variant takes place. The insets (a) and (b) of figure 4 present the optical micrographs of the surface of the $Co_{47.5}Ni_{22.5}Ga_{30.0}$ before and after applying compressive stress, respectively. Before applying stress as seen from (a), a clear surface relief pattern is observed, indicating that the martensite phase of the present specimen is in a multi-variant state. After applying stress, the surface relief pattern completely vanishes as shown in (b). These results indicate that the stress facilitates the growth of specific oriented variants, resulting in a single-variant state in which the *c*-axis is oriented to the $[001]_P$ direction. In order to evaluate the variant boundary mobility, the compressive stress was applied along the $[001]_P$ direction, i.e. the *c*-axis direction, of the single-variant specimen in the second cycle. The variant rearrangement occurs at a stress level of 12–15 MPa. The residual strain is estimated to be 14.8 % from figure 4. On the other hand, the calculated residual strain from the lattice parameters in figure 2 is 17.1 %, when the specimen changes from one single-variant into another single-variant state. The stress–strain curve was measured at room temperature, whereas the x-ray diffraction measurement was carried out at 100 K because of the phase stability, as described in section 3.1. The strain calculated from the lattice constants is reduced with increasing temperature in Co–Ni–Ga [26]. The difference in magnitude of the residual strains between the experimental and the calculated values would be attributed to the difference in the experimental temperatures.

3.3. Magnetic anisotropy constant

Presented in figure 5 are the magnetization curves (M–H) as a function of temperature for the single-variant $Co_{47.5}Ni_{22.5}Ga_{30.0}$ in the martensite phase. The magnetic field was applied along the *c*-axis ($[001]_P$) and $[110]_M$ or $[\bar{1}10]_M$ ($[100]_P$ or $[010]_P$) of the $L1_0$ structure. The measured M–H curve for the $[110]_M$ or $[\bar{1}10]_M$ is easily saturated, while the curve for the *c*-axis is hardly saturated below 13 kOe. These results tell us that the *c*-axis is regarded as the hard axis. In order to determine the saturation magnetization M_{sat}, the law of approach to saturation was applied to the experimental data from $H = 8$ to 50 kOe [29]. The magnetic anisotropy energy

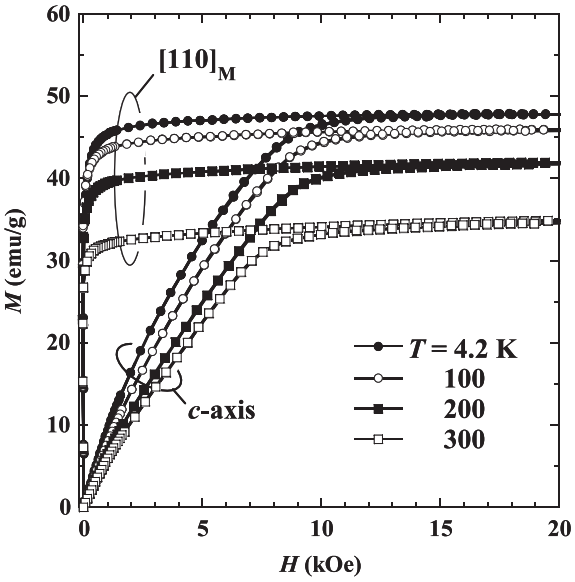

Figure 5. Magnetization curves along the *c*-axis and $[110]_M$ as a function of temperature for the single-variant $Co_{47.5}Ni_{22.5}Ga_{30.0}$.

E_{MAE} in the uniaxial symmetry systems depends on the angle θ between the magnetization and the *c*-axis:

$$E_{MAE} \cong K_{u1}\sin^2\theta + K_{u2}\sin^4\theta, \qquad K_u \cong K_{u1} + K_{u2} \quad (1)$$

where K_{u1} and K_{u2} are magnetic anisotropy constants [30]. After correcting the demagnetizing field, K_{u1}, K_{u2}, and $K_{u1} + K_{u2}$ are evaluated by the following Sucksmith–Thompson method [31].

$$\frac{H_{eff}}{M} = 2K_{u1}\frac{1}{M_{sat}^2} + 4K_{u2}\frac{M^2}{M_{sat}^4}. \quad (2)$$

Accordingly, the magnetic anisotropy constants can be evaluated by plotting in the form of M^2 and H/M, the slope being $4K_{u2}/M_{sat}^4$ and the intercept $2K_{u1}/M_{sat}^2$. The plots of M^2 against H/M for the magnetization curve along the *c*-axis at 4.2 K from $H = 3$ to 8 kOe are presented in the inset of figure 6 for the single-variant $Co_{47.5}Ni_{22.5}Ga_{30.0}$. From the present data in the inset of figure 6, K_{u1}, K_{u2}, and $K_{u1} + K_{u2}$ at 4.2 K are evaluated to be -1.11×10^6, -0.41×10^6, and -1.52×10^6 erg cm^{-3}, respectively. Similar analyses were carried out using the data measured at several different temperatures. The temperature dependences of the saturation magnetization M_{sat} and the magnitude of uniaxial magnetic anisotropy constant $|K_u|$ which stands for $|K_{u1} + K_{u2}|$ for the single-variant $Co_{47.5}Ni_{22.5}Ga_{30.0}$ in the martensite phase are depicted in figure 6. Both M_{sat} and $|K_u|$ of the martensite phase decrease with increasing temperature up to T_C as seen from figure 6. The values of K_{u1}, K_{u2}, and $K_{u1} + K_{u2}$ for $Co_{47.5}Ni_{22.5}Ga_{30.0}$ at $T = 300$ K are evaluated to be -0.98×10^6, -0.09×10^6 and -1.07×10^6 erg cm^{-3}, respectively.

3.4. Magnetic-field-induced strain

The variant rearrangement driven by magnetic field has been discussed quantitatively by introducing the magnetic shear

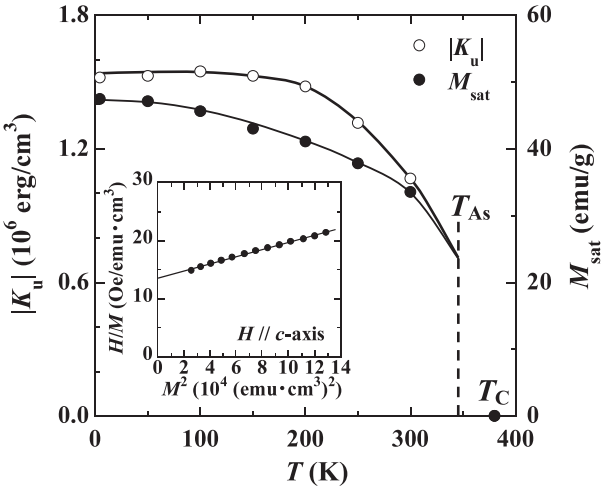

Figure 6. Temperature dependence of the saturation magnetization M_{sat} and the magnitude of the magnetic anisotropy constants $|K_u|$ for the martensite of the single-variant $Co_{47.5}Ni_{22.5}Ga_{30.0}$. The inset shows the plot in the form of M^2 against H/M for magnetization along the c-axis at 4.2 K from $H = 3$ to 8 kOe for the single-variant $Co_{47.5}Ni_{22.5}Ga_{30.0}$.

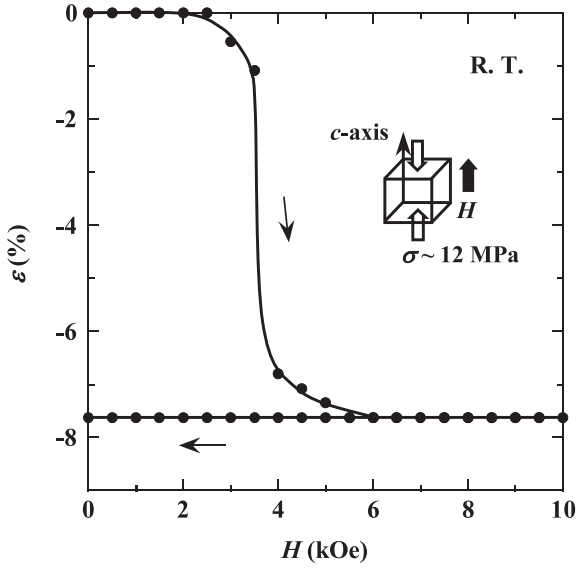

Figure 7. MFIS measured parallel to the direction of magnetic field H applied along the c-axis at room temperature under a stress of about 12 MPa for the single-variant $Co_{47.5}Ni_{22.5}Ga_{30.0}$.

stress τ_{mag} acting across the twinning plane [32]. In order to satisfy the condition for the variant rearrangement by applying magnetic field, τ_{mag} should be larger than the mechanical shear stress τ_{req} required for the variant rearrangement. In other words, the following criterion should be satisfied:

$$|K_u|/s = \tau_{mag} > \tau_{req}. \quad (3)$$

The value of τ_{mag} is expressed as $|K_u|/s$, where s is the corresponding twinning shear. The twinning plane is $\{101\}_P$ for the Co–Ni–Ga system, therefore the twinning shear is expressed as

$$s = \{1 - (c/a)^2\}/(c/a). \quad (4)$$

The value of s is calculated to be 0.360 by using the lattice parameter ratio $c/a = 0.836$ obtained from figure 2. The value of $|K_u|$ at 300 K is estimated to be 1.07×10^6 erg cm^{-3} from figure 6. Therefore, the value of τ_{mag} is evaluated to be 0.3 MPa. The twinning plane is $\{101\}_P$ for the $Co_{47.5}Ni_{22.5}Ga_{30.0}$ alloy, therefore, the corresponding shear stress required for the rearrangement of variant τ_{req} is obtained by considering the Schmid factor for the $\{101\}_P$ twinning mode. The Schmid factor for the primary slip system is 0.5 in this case, then τ_{req} ($=0.5\sigma_{tw}$) is estimated to be 6.0–7.5 MPa from the applied twinning stress σ_{tw} (=12–15 MPa) in figure 4. As it turns out, the magnitude of shear stress becomes $\tau_{mag} < \tau_{req}$ and is not satisfied by the condition given by equation (3). Consequently, no MFIS is obtained in the present alloy. In the $L1_0$ structure, a high twinning stress needs to induce the twinning transformation, and hence such high twinning stress hinders the appearance of large MFIS.

To obtain a large MFIS, in other words, to satisfy the appearance condition of MFIS ($\tau_{mag} > \tau_{req}$), a static stress was used to assist the τ_{mag}. To be more concrete, the magnetic field was applied under a compressive stress. Before applying magnetic field, a compressive stress of about 12 MPa was applied along the c-axis hard magnetic direction. The compressive stress is converted to a shear stress of 6 MPa by using the Schmid factor of 0.5. The magnetic field was then applied parallel to the c-axis direction. That is, the assisted shear stress $\tau_{assist} = 6$ MPa was first applied, and then the magnetic shear stress τ_{mag} of about 0.3 MPa was added by applying magnetic field in addition to τ_{assist}. There is a plateau in the stress–strain curve as shown in figure 4, corresponding to $\tau_{req} = 6.0$–7.5 MPa ($\sigma_{tw} = 12$–15 MPa). By applying assisted and magnetic shear stresses, therefore, the strain corresponding to the total applied shear stress $\tau_{assist} + \tau_{mag} = 6.3$ MPa is obtained. As a result, as shown in figure 7, during applying magnetic field, a steep shrinkage caused by the variant rearrangement is observed around $H = 4$ kOe, and the maximal strain of 7.6 % is achieved in a magnetic field of 10 kOe. The thin solid arrows indicate the increasing and decreasing magnetic field processes. The inset of figure 7 shows the relation among the sample orientation and the applied compressive stress and magnetic field directions. The thick open and solid arrows stand for the stress and the magnetic field directions, respectively.

4. Conclusion

From the thermomagnetization and differential scanning calorimetric curves, several temperatures are defined as follows: the Curie temperature $T_C = 380$ K, the martensitic transformation starting temperature $T_{Ms} = 337$ K, its finishing temperature $T_{Mf} = 332$ K, the reverse transformation starting temperature $T_{As} = 344$ K, and its finishing temperature $T_{Af} = 352$ K in $Co_{47.5}Ni_{22.5}Ga_{30.0}$ single crystal. In the compressive test at room temperature, the residual strain of 14.8 % was observed under a twinning stress level of 12–15 MPa. The single-variant state was established after applying compressive stress. The c-axis was determined to

be the magnetic hard axis from the magnetization curves. In the single-variant $Co_{47.5}Ni_{22.5}Ga_{30.0}$ β' martensite phase, the magnetic anisotropy constants K_{u1}, K_{u2}, and $K_{u1} + K_{u2}$ estimated by the Sucksmith–Thompson method are -0.98×10^6, -0.09×10^6, and -1.07×10^6 erg cm^{-3} at 300 K, respectively. Since no sufficiently large value of the MFIS was observed, the magnetic field was applied under a compressive stress to achieve a large MFIS. It follows that a large MFIS of about 7.6 % was obtained in the martensite phase at room temperature under a static compressive stress of about 12 MPa for the single-variant $Co_{47.5}Ni_{22.5}Ga_{30.0}$.

Acknowledgments

The authors wish to thank Professor Y Sutou, and Messrs T Ota and C Saito for their experimental support. A part of the present study was supported by the Ministry of Education, Culture, Sports Science, and Technology, Japan, and the Grant-in-Aids for Scientific Research, Core Research for Evolutional Science and Technology (CREST) and the Research Fellow of the Japan Society.

References

[1] Ullakko K, Huang J K, Kantner C, O'Handley R C and Kokorin V V 1996 *Appl. Phys. Lett.* **69** 1966
[2] O'Handley R C 1998 *J. Appl. Phys.* **83** 3263
[3] Heczko O, Sozinov A and Ullakko K 2000 *IEEE Trans. Magn.* **36** 3266
[4] Murray S J, Marioni M, Allen S M, O'Handley R C and Lograsso T A 2000 *Appl. Phys. Lett.* **77** 886
[5] Sozinov A, Likhachev A A, Lanska N and Ullakko K 2002 *Appl. Phys. Lett.* **80** 1746
[6] Sozinov A, Likhachev A A and Ullakko K 2002 *IEEE Trans. Magn.* **38** 2814
[7] James R D and Wuttig M 1998 *Phil. Mag.* A **77** 1273
[8] Kakeshita T, Takeuchi T, Fukuda T, Tsujiguchi M, Saburi T, Oshima R and Muto S 2000 *Appl. Phys. Lett.* **77** 1502
[9] Fujita A, Fukamichi K, Gejima F, Kainuma R and Ishida K 2000 *Appl. Phys. Lett.* **77** 3054
[10] Oikawa K, Wulff L, Iijima T, Gejima F, Ohmori T, Fujita A, Fukamichi K, Kainuma R and Ishida K 2001 *Appl. Phys. Lett.* **79** 3290
[11] Morito H, Fujita A, Fukamichi K, Kainuma R, Ishida K and Oikawa K 2002 *Appl. Phys. Lett.* **81** 1657
[12] Oikawa K, Ota T, Sutou Y, Ohmori T, Kainuma R and Ishida K 2002 *Mater. Trans.* **43** 2360
[13] Oikawa K, Ota T, Ohmori T, Tanaka Y, Morito H, Fujita A, Kainuma R, Fukamichi K and Ishida K 2002 *Appl. Phys. Lett.* **81** 5201
[14] Morito H, Fujita A, Fukamichi K, Kainuma R, Ishida K and Oikawa K 2003 *Appl. Phys. Lett.* **83** 4993
[15] Sutou Y, Kamiya N, Omori T, Kainuma R, Ishida K and Oikawa K 2004 *Appl. Phys. Lett.* **84** 1275
[16] Kainuma R, Imano Y, Ito W, Sutou Y, Morito H, Okamoto S, Kitakami O, Oikawa K, Fujita A, Kanomata T and Ishida K 2006 *Nature* **439** 957
[17] Morito H, Fujita A, Oikawa K, Ishida K, Fukamichi K and Kainuma R 2007 *Appl. Phys. Lett.* **90** 062505
[18] Wuttig M, Li J and Craciunescu C 2001 *Scr. Mater.* **44** 2393
[19] Oikawa K, Ota T, Gejima F, Ohmori T, Kainuma R and Ishida K 2001 *Mater. Trans.* **42** 2472
[20] Chernenko V A, Pons J, Cesari E and Perekos A E 2004 *Mater. Sci. Eng.* A **378** 357
[21] Craciunescu C, Kishi Y, Lograsso T A and Wuttig M 2002 *Scr. Mater.* **47** 285
[22] Chernenko V A, Pons J, Cesari E and Zasimchuk I K 2004 *Scr. Mater.* **50** 225
[23] Sato M, Okazaki T, Furuya Y, Kishi Y and Wuttig M 2004 *Mater. Trans.* **45** 204
[24] Li Y X, Liu H Y, Meng F B, Yan L Q, Liu G D, Dai X F, Zhang M, Liu Z H, Chen J L and Wu G H 2004 *Appl. Phys. Lett.* **84** 3594
[25] Dai X F, Liu G D, Liu Z H, Wu G H, Chen J L, Meng F B, Liu H Y, Yan L Q, Qu J P, Li Y X, Wang W G and Xiao J Q 2005 *Appl. Phys. Lett.* **87** 112504
[26] Brown P J, Ishida K, Kainuma R, Kanomata T, Neumann K-U, Oikawa K, Ouladdiaf B and Ziebeck K R A 2005 *J. Phys.: Condens. Matter* **17** 1301
[27] Kainuma R, Ise M, Jia C-C, Ohtani H and Ishida K 1996 *Intermetallics* **4** S151
[28] Nishiyama Z 1971 *Martensitic Transformation* (Tokyo: Maruzen) pp 204–8
[29] Chikazumi S 1997 *Physics of Ferromagnetism* 2nd edn (New York: Oxford Science Publications) pp 467–517
[30] O'Handley R C 2000 *Modern Magnetic Materials* (New York: Wiley) pp 179–217
[31] Sucksmith W and Thompson J E 1954 *Proc. R. Soc.* A **225** 362
[32] Kakeshita T and Fukuda T 2006 *Sci. Technol. Adv. Mater.* **7** 350